3D metal powder additive manufacturing phased array antenna for multichannel Doppler reflectometer

Review of Scientific Instruments

3D metal powder additive manufacturing phased array antenna for multichannel Doppler reflectometer

Cite as: Rev. Sci. Instrum. **93**, 113535 (2022); https://doi.org/10.1063/5.0101723
Submitted: 03 June 2022 • Accepted: 07 September 2022 • Published Online: 14 November 2022

T. Tokuzawa, T. Nasu, S. Inagaki, et al.

AIP Publishing

Review of Scientific Instruments ARTICLE scitation.org/journal/rsi

3D metal powder additive manufacturing phased array antenna for multichannel Doppler reflectometer

Cite as: Rev. Sci. Instrum. 93, 113535 (2022); doi: 10.1063/5.0101723
Submitted: 3 June 2022 • Accepted: 7 September 2022 •
Published Online: 14 November 2022

T. Tokuzawa,[1,2,a)] T. Nasu,[2] S. Inagaki,[3] C. Moon,[4] T. Ido,[4] H. Idei,[4] A. Ejiri,[5] R. Imazawa,[6] M. Yoshida,[6] N. Oyama,[6] K. Tanaka,[1,4] and K. Ida[1,2]

AFFILIATIONS

[1] National Institute for Fusion Science, National Institutes of Natural Sciences, Toki 509-5292, Japan
[2] The Graduate University for Advanced Studies, SOKENDAI, Toki 509-5292, Japan
[3] Institute of Advanced Energy, Kyoto University, Gokasho, Uji 611-0011, Japan
[4] Research Institute for Applied Mechanics, Kyushu University, Kasuga 816-8580, Japan
[5] Graduate School of Frontier Sciences, The University of Tokyo, Kashiwa 277-8561, Japan
[6] National Institutes for Quantum Science and Technology, 801-1 Mukoyama, Naka, Ibaraki 311-0193, Japan

Note: This paper is part of the Special Topic on Proceedings of the 24th Topical Conference on High-Temperature Plasma Diagnostics.
[a)] **Author to whom correspondence should be addressed:** tokuzawa@nifs.ac.jp

ABSTRACT

Measuring the time variation of the wavenumber spectrum of turbulence is important for understanding the characteristics of high-temperature plasmas, and the application of a Doppler reflectometer with simultaneous multi-frequency sources is expected. To implement this diagnostic in future fusion devices, the use of a phased array antenna (PAA) that can scan microwave beams without moving antennas is recommended. Since the frequency-scanning waveguide leaky-wave antenna-type PAA has a complex structure, we have investigated its characteristics by modeling it with 3D metal powder additive manufacturing (AM). First, a single waveguide is fabricated to understand the characteristics of 3D AM techniques, and it is clear that there are differences in performance depending on the direction of manufacture and surface treatment. Then, a PAA is made, and it is confirmed that the beam can be emitted in any direction by frequency scanning. The plasma flow velocity can be measured by applying the 3D manufacturing PAA to plasma measurement.

I. INTRODUCTION

In the study of energy cascades and entropy transport in plasma turbulence, it is important to measure the temporal changes in the wavenumber spectrum of turbulence in high-temperature plasmas. The Doppler reflectometer allows non-contact local observation of the wavenumber spectrum by scanning the incident angle to the plasma[1,2] and is expected to apply to a fusion reactor. However, there are many issues to be considered for the operation of the antenna drive mechanism in the restricted environment of a vacuum vessel, including its maintainability. Therefore, in this study, we investigated the application of a phased array antenna (PAA) based method, which can change the direction of the microwave beam without using a steering mechanism, to a plasma experimental device. In particular, we expect that a PAA, in combination with a frequency comb-based Doppler reflectometer,[3,4] will enable us to measure simultaneous beam emission in multiple directions and time variations of the wavenumber spectrum.

The PAA enables the radiation of electromagnetic waves in any direction by maintaining a constant spacing d between antennas arranged in an array, as shown in Fig. 1. When the waveguide is used as a transmission line, the waveguide spacing length is l, and the wavenumber in the waveguide is k_g, the radiation angle θ is

$$\theta = \sin^{-1}\left(-\frac{k_g}{k}\frac{l}{d}\right), \tag{1}$$

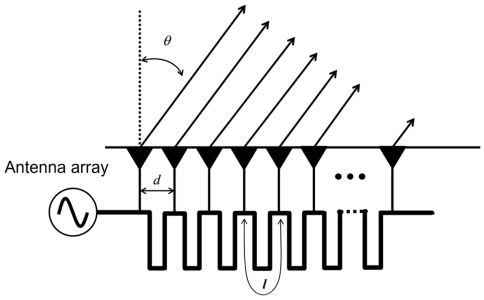

FIG. 1. Principle of phased array antenna radiation.

which enables beam radiation at a wide angle. Here, k is the wavenumber of the incident wave. The phase difference between antennas changes automatically when the incident frequency is changed, eliminating the need for additional phase control equipment and allowing for a simple structure design. This type of PAA is also called a frequency-scanning waveguide array.[5–7]

When designing a PAA, we need to be concerned about the grating lobe, which affects the directivity of the antenna. The condition for avoiding grating lobes is

$$\frac{d}{\lambda} < \frac{1}{1 + |\sin\theta^{\max}|}. \tag{2}$$

Here, λ is the wavenumber of the incident wave, and $\theta^{\max}$ is the maximum radiation angle. For example, when $\theta^{\max} = 20°$, $d < 12.5$ mm for the Ku-band, and $d < 4.5$ mm for the Q-band.

Among PAA designs, the waveguide leaky-wave antenna (WLA) array is a suitable one because of its ability to generate a linear polarized wave, which is an advantage for measuring magnetized confinement plasma. On the other hand, the WLA array requires a complicated three-dimensional helical structure. In the reference work,[8] electroforming (EF) techniques were used for fabrication. EF is an excellent technology, and assembled antennas are known to perform well in the millimeter wave band; however, the relatively high manufacturing cost makes it unsuitable for experimentation with various antenna designs. Therefore, in this study, we make antennas using a recent innovative metal powder additive manufacturing (AM) technique and using a so-called 3D metal printer.[9,10] This has two advantages: (1) it allows us to experiment with various antenna designs at a relatively low cost and (2) it allows us to produce antennas in a variety of metal materials.

However, due to the rough surface of AM manufacturing, there is some uncertainty as to whether the 3D printed model can be used for plasma measurement. Therefore, here, we report the results of constructing a waveguide and PAA using a 3D printer, investigating their performance, and applying them to a plasma experiment.

II. 3D METAL ADDITIVE MANUFACTURING CHARACTERISTICS

To characterize the creation by 3D metal additive manufacturing, we first fabricate two types of waveguides and investigate two of these characteristics. One is the difference in characteristics due to the orientation of the manufacturing process. The other is the difference due to the surface treatment method.

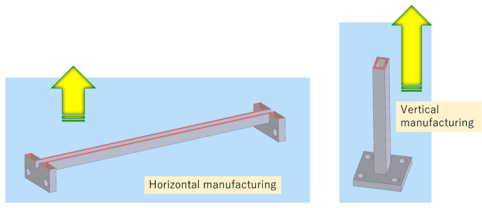

FIG. 2. Schematic drawing of manufacturing direction. The products are manufactured by stacking them horizontally (left) and vertically (right) as indicated by the arrows.

A. Difference in the manufacturing direction

Ku-band (12.4–18.0 GHz) waveguides are produced by a selective laser melting (SLM) 3D printer (SLM280PS), which is used to melt a copper powder (C18150) to form layers every 30 μm. When using 3D manufacturing, it is necessary to choose in which direction to stack. In the case of waveguide fabrication, there is an option to construct horizontally or vertically, as shown in Fig. 2. The target for the surface roughness of the waveguides is Ra (arithmetic mean estimate) 3.2–6.3 μm, which is equivalent to that of commercial products. The measured values of the assembled waveguides are Ra = 4.42–5.57 μm for vertical manufacturing and Ra > 5.76 μm for horizontal manufacturing. It should be noted that in horizontal manufacturing, there are areas where the surface roughness is too large to measure.

Figure 3 shows the transmission characteristics through 110 mm long Ku-band waveguides measured with a vector network analyzer (VNA). It is confirmed that Ku-band microwaves can be transmitted in both waveguides with a loss of less than 0.5 dB. Compared to the commercial waveguide, the difference is small for the vertical manufacturing waveguide, but for the horizontal manu-

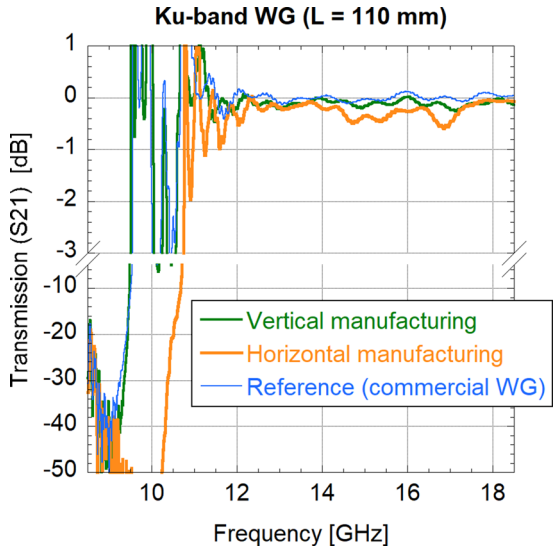

FIG. 3. Transmission characteristics of Ku-band waveguides assembled in vertical (green) and horizontal (orange) manufacturing directions and commercial waveguides (blue) for reference.

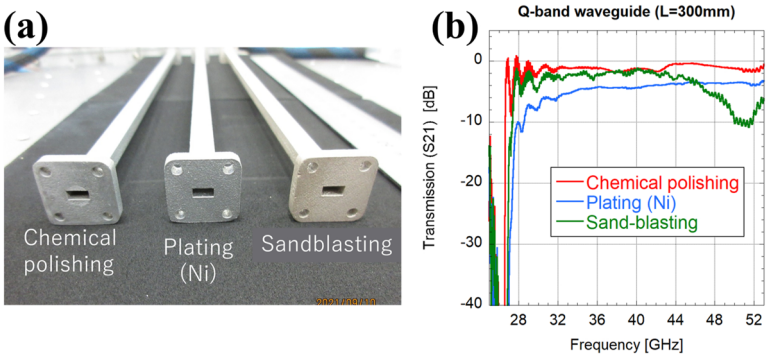

FIG. 4. (a) Photograph of Q-band aluminum waveguides. (b) Transmission characteristics of Q-band waveguides. Each surface is treated by sandblasting (green), nickel plating (blue), and chemical polishing (red).

facturing case, the transmission loss is slightly larger, and the cutoff frequency is also higher. This is because the ceiling section loses its support during fabrication, causing it to sag. This is consistent with a narrower inner dimension of the waveguide and a higher cutoff frequency. In fact, in this example, the cutoff frequency increased from 9.5 to 10.7 GHz, and the average value is estimated to be about 14.0 mm, down from the design value of 15.8 mm. Incidentally, the smallest value measured is 13.5 mm. This also indicates that the frequency response of the propagation can be examined to determine the internal conditions. A copper waveguide 300 mm long was also made, and the total transmission loss with this method is estimated to be 0.8 dB/m.

B. Difference in surface treatment

Next, we investigate how performance changes if this surface is subjected to a smoothing treatment. Q-band (33–50 GHz) waveguides modeled in aluminum are subjected to three different surface treatments: sandblasting, nickel (Ni) plating, and chemical polishing. Since the inner surface of the waveguide is important in terms of performance, the effects of higher frequency bandwidth and smaller waveguide size than in Sec. II A is investigated, making the process more difficult. The SLM type 3D metal printer is also used to melt aluminum alloy powder (ALSi10Mg) and fabricated 300 mm Q-band waveguides. A photograph after surface treatment is shown in Fig. 4(a). Transmission performances of waveguides are measured by the VNA, and the results are shown in Fig. 4(b). Transmission loss is found to increase in the order of chemical polishing, sandblasting, and Ni plating. The cutoff frequency in the case of Ni plating is higher than the others. Therefore, in the case of Ni plating, there may be a problem with the treatment of the inner part of the waveguide. The total transmission loss after the chemical polishing treatment is estimated to be about 6 dB/m. Since this value is greater than 1 dB/m of commercial waveguides, it is indicated that AM waveguides are available, but the length used should be limited to the appropriate distance.

III. PHASED ARRAY ANTENNA (PAA)

Two bands of PAAs of different metallic materials are made to investigate the effects of both the number of turns and surface treatment. Unlike waveguide fabrication, PAA fabrication cannot be performed in completely vertical manufacturing, and AM fabrication was performed at a 45° tilt.

A. Effect of turn number tested by copper PAA in Ku-band

First, as a prototype, a Ku-band WLA-type PAA with three turns is designed with a distance of 12.4 mm between WLA apertures and a turn diameter of 118 mm, as shown in Fig. 5(a). It is produced using copper powder (C18150). After examining its radiation characteristics as a PAA, we cut it to measure its inner surface roughness. The measured Ra is found to be 12.5–25 μm, which is

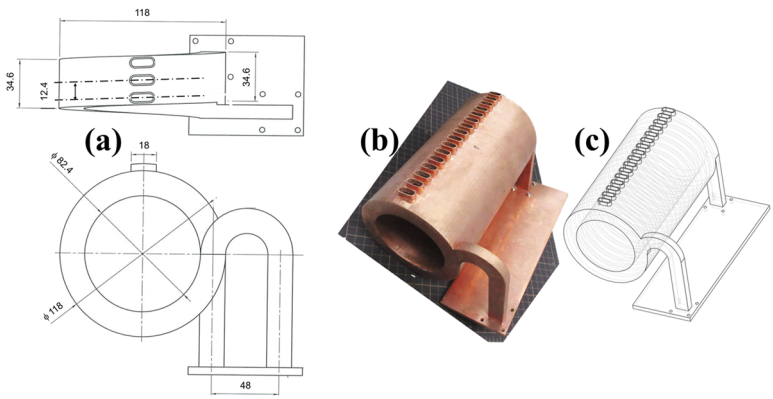

FIG. 5. (a) Designed drawing of three-turn copper Ku-band WLA PAA. (b) Photograph and (c) design sketch of 16-turn WLA PAA. The distance of each aperture and winding radius are the same in both three-turn and 16-turn antennae.

four times larger than the target value of 3.2–6.3 μm. However, the surface roughness is still less than 1/1000 of the wavelength, and the radiation from the antenna can be observed, as shown in Fig. 6(b).

Then, a 16-turn WLA PAA is constructed to compare the performance of a different number of turns, as shown in Figs. 5(b) and 5(c). The radiation distribution is examined to determine whether the radiation direction can be controlled by frequency, which is the key to the performance of this PAA. Figure 6(a) shows the frequency dependence of the radiation intensity. Here, the radiation pattern is measured by rotating the PAA antenna and placing the horn antenna on the opposite side as a receiver. The peak frequency moves by changing the angle of the antenna, confirming that the radiation direction can be controlled by frequency. The reason why the peak frequency appears periodically at each radiation angle is that k_g/k varies with frequency on the right-hand side of Eq. (1), allowing radiation in the same radiation direction every 2π in sin. In the case of three turns, the change in radiation direction (directivity) due to this frequency change is not clear, but in the case of 16 turns, a clear change is observed.

B. Effect of surface treatment tested by aluminum PAA in Q-band

The effects of different surface treatments after manufacturing are also investigated in PAA. The base PAA is a Q-band, six-turn structure produced using aluminum powder. With a turn diameter of 100 mm and aperture spacing of 6.25 mm, a radiation angle of ~20° is possible on the long wavelength side of the Q-band. Three different surface treatments have been attempted for the PAA. It has a tapered aperture horn integrally constructed from the aperture of the WLA.

Figure 7(a) shows the radiation characteristics of these PAAs. The property of being able to change the direction of radiation by varying the frequency is not significantly different for any surface-treatment PAA, but the performance is slightly lower for the Ni-plating case in terms of radiation intensity and directivity. In addition, the frequencies at which the radiation intensity peaks in a defined direction are shifted in the order of sand-blasting, chemical-polishing, and Ni-plating. This can be attributed to the fact that the wavenumber in the waveguide is affected by the size of the inside of the waveguide due to the different surface treatments, as seen in Fig. 4(b).

As shown in Fig. 7(b), the radiation direction can vary continuously with the input frequency. In this case, a slight difference in frequency of 0.2 GHz changes the angle by about 20°. When applied to a Doppler reflectometer, this means that the turbulence with different wavenumbers can be observed at almost the same cutoff layer because the incident frequency is almost the same. Therefore, if multi-frequency oscillation is performed at the same time as a probe, simultaneous multi-directional radiation is possible, and the ability to measure the time variation of the wavenumber spectrum is expected.

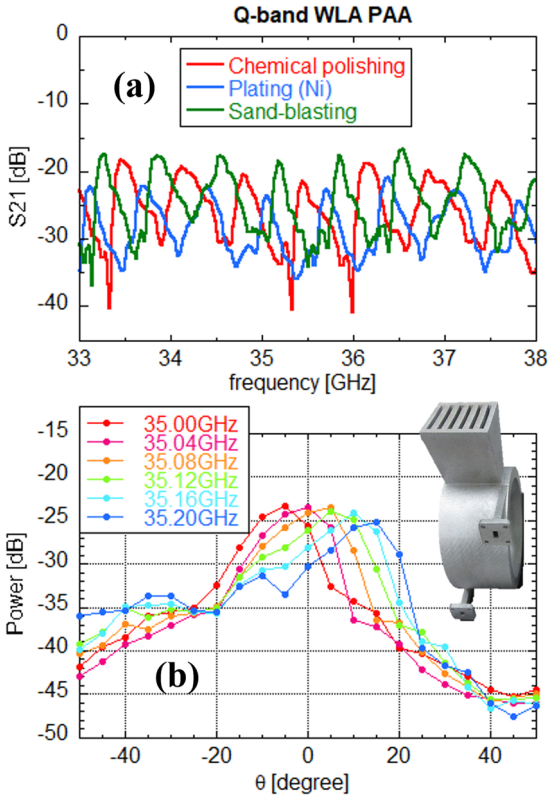

FIG. 7. (a) Frequency dependence of radiated power received by a horn antenna 200 mm away from the Q-band PAA and (b) radiation distribution in the chemical polished PAA. In this frequency range, microwaves can be radiated in different directions over a range of about ±10°.

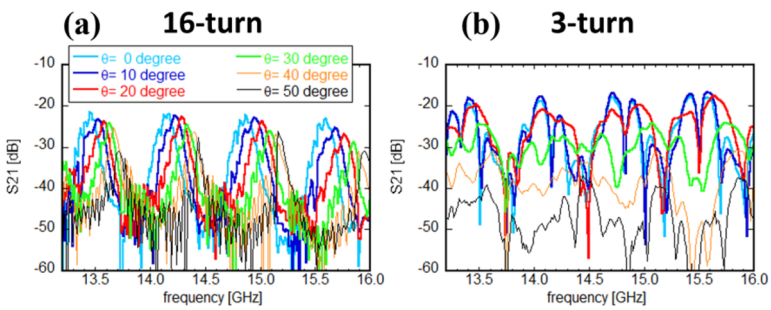

FIG. 6. PAA directivity test. Frequency dependence of radiated power received by a horn antenna 200 mm away from the PAA for (a) 16-turn PAA and (b) three-turn PAA. Here, the difference in color means the angle between the angle-scanned PAA and the receiving horn antenna.

IV. PAA APPLICATION FOR DOPPLER REFLECTOMETER IN PANTA PLASMA

After confirming on a test bench that the WLA PAA can radiate microwave beams in any direction without driving an antenna steering mechanism, a Doppler reflectometer (Ku-band) using this developed PAA was installed in a trial to measure the plasma flow velocity in Plasma Assembly for Nonlinear Turbulence Analysis (PANTA).[11,12] PANTA is the plasma experimental device that has a vacuum vessel with a diameter of 450 mm and an axial length of 4 m and generates plasma with a diameter of about 100–120 mm. A Ku-band WLA PAA was placed in the horizontal position of the PANTA with an accuracy of less than 2 mm vertically, using a laser marking device to allow vertical scanning of the plasma. The heterodyne Doppler reflectometer was provided as the measurement system. The +18 dBm output from the microwave generator (Anritsu: MG3692C) was used as the source and input to the PAA via a circulator, and the microwaves emitted from PAA were used as the probe beam. The same port of the PAA received the scattered wave and directed it through the circulator to the RF port of the mixer. A frequency-adjusted +12 dBm output with a beat frequency of exactly 1 MHz was used for the local wave of the mixer. The intermediate frequency (IF) signal, which was the mixer output, was then captured by the oscilloscope with a sampling rate of 25 MS/s and ten MSample data points.

The plasma experiment was performed in a magnetic field of 900 Gauss, an argon gas pressure of 5 mTorr, and a plasma created by 7 MHz, and 3 kW helicon waves. The launching frequency was changed on a shot-by-shot basis. A clear Doppler shift was observed in the frequency spectrum of the scattered signal. Fast Fourier transform (FFT) processing was performed for every 2^{18} points (frequency resolution was 95 Hz) at a stable 200 ms time during the discharge, and the Doppler shift was obtained from the average of the FFT calculations and plotted for each incident frequency in Fig. 8. It is confirmed that the Doppler shift frequency varies almost linearly in this frequency scan range. From the variation of the angle of incidence for each frequency, the measured position of the plasma and the wavenumber could be determined. The plasma flow can then be estimated from this to be 8–12 m/s, which is not significantly inconsistent with previous electrostatic probe measurements.

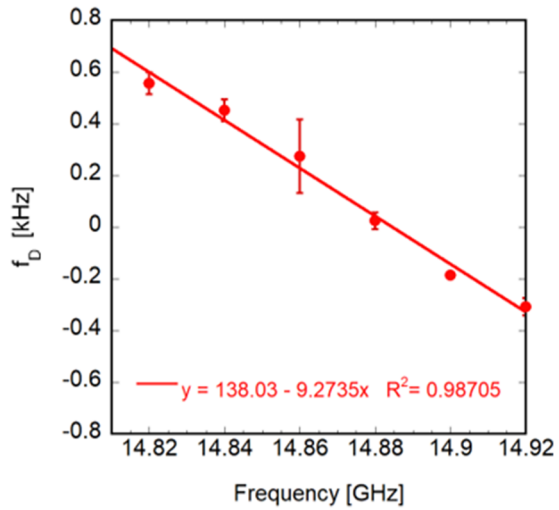

FIG. 8. Frequency dependence of Doppler shift when the probe frequency is around 15 GHz.

V. SUMMARY

Waveguides and PAA antennas are designed and made by 3D metal powder additive manufacturing, and the following results are obtained: (1) The surface roughness of the fabricated waveguide varies depending on the direction of the construction process, and the performance of the manufactured waveguide differs. (2) Surface treatment (especially "chemical polishing" or "sandblasting") after modeling is effective. (3) The manufactured WLA-type PAAs can radiate microwave beams in any direction by controlling the frequency. (4) The Doppler radar using the PAA could be applied to plasma flow velocity diagnostics.

In the future, we plan to use such a PAA to challenge the observation of time variations of the scattering wavenumber spectrum of turbulence in high-temperature plasmas, such as JT-60SA and DEMO.

ACKNOWLEDGMENTS

The author expresses special thanks to Mr. T. Miyazaki of TKE Co., LTD. and Mr. Y. Sayama of DOHO Corporation for their assistance in the production of the 3D modeling. This work was supported, in part by, KAKENHI (Grant Nos. 19H01880 and 21H04973), a budgetary Grant-in-Aid from the NIFS LHD project under the auspices of the NIFS Collaboration Research Program (Grant No. ULPP027), and the collaboration programs of the RIAM of Kyushu University and the QST institute.

AUTHOR DECLARATIONS

Conflict of Interest

The authors have no conflicts to disclose.

Author Contributions

T. Tokuzawa: Conceptualization (lead); Formal analysis (lead); Funding acquisition (lead); Investigation (lead); Project administration (equal); Resources (equal); Writing – original draft (lead). **N. Oyama**: Project administration (supporting); Writing – review & editing (equal). **K. Tanaka**: Conceptualization (supporting); Writing – review & editing (equal). **K. Ida**: Supervision (equal); Writing – review & editing (equal). **T. Nasu**: Data curation (equal); Formal analysis (equal); Investigation (equal). **S. Inagaki**: Conceptualization (equal); Investigation (equal); Resources (equal); Validation (equal). **C. Moon**: Data curation (equal); Formal analysis (equal); Investigation (equal); Resources (equal); Validation (equal). **T. Ido**: Resources (equal); Validation (equal). **H. Idei**: Conceptualization (equal); Writing – review & editing (equal). **A. Ejiri**: Conceptualization (equal); Writing – review & editing (equal). **R. Imazawa**: Conceptualization (equal); Project administration (equal); Writing – review & editing (equal). **M. Yoshida**: Project administration (equal); Writing – review & editing (equal).

DATA AVAILABILITY

The data that support the findings of this study are available from the corresponding author upon reasonable request.

REFERENCES

[1]L. Vermare *et al.*, Phys. Plasmas **18**, 012306 (2011).
[2]T. Happel *et al.*, Plasma Phys. Controlled Fusion **59**, 054009 (2017).
[3]T. Tokuzawa *et al.*, Plasma Fusion Res. **9**, 1402149 (2014).
[4]T. Tokuzawa *et al.*, Appl. Sci. **12**(9), 4744 (2022).
[5]A. Ishimaru and H.-S. Tuan, IEEE Trans. Antennas Propag. **10**(2), 144 (1962).
[6]J. Hilburn and F. Prestwood, IEEE Trans. Antennas Propag. **22**(2), 340 (1974).
[7]W. Yin *et al.*, IEEE Access **8**, 77245 (2020).
[8]T. Windisch *et al.*, Rev. Sci. Instrum. **89**, 10H115 (2018).
[9]S. B. Korsholm *et al.*, Rev. Sci. Instrum. **92**, 033509 (2021).
[10]A. H. Seltzman and S. J. Wukitch, Fusion Eng. Des. **159**, 111762 (2020).
[11]T. Yamada *et al.*, Nucl. Fusion **54**, 114010 (2014).
[12]T. Inagaki *et al.*, Sci. Rep. **6**, 22189 (2016).